Energy Proceedings
Vol 45, 2024
ISSN 2004-2965

Exploring Direct Parabolic Trough Supercritical Brayton Cycle with Direct Contact Membrane Distillation (DCMD) for co-generation of Power and Water.

Hafiz Aman Zaharil[1*], Hong-xing Yang[1]

1 Renewable Energy Research Group (RERG), Department of Building Environment and Energy Engineering, The Hong Kong Polytechnic University, Hong Kong.

(*Corresponding Author: hafiz.binamanzaharil@connect.polyu.hk)

ABSTRACT

The quest for energy sustainability and clean water is at the forefront of humanity's challenge today. This research aims to utilize an integration of parabolic trough solar power plant with sCO_2 Brayton cycle coupled with a direct contact desalination system. An integrated model was developed to achieve the aim. The results illustrated that thermal and exergetic efficiency increased with Pressure Ratio (PR) increment and peaked at around PR of 3.2 and decreased thereafter. The change in net work output (ΔW_{net}), transitioning from 101 kW to 7 kW as PR increases from 2.7 to 3.2, indicates a reducing rate of increment. However, from PR 3.2 to 3.7, ΔW_{net} showed negative values, from -1 kW to -74 kW, reflecting not only reducing efficiencies, but also an increasing rate of its reduction. Increasing the bottoming cycle pressure continuously reduces efficiency, with minor declines between pressures of 7400 to 7600 kPa due to sCO_2 density changes near the critical point. Furthermore, the interplay between pressure ratio (PR) and the bottoming cycle (P1) affects both water production and the number of DCMD units required. Water production and DCMD units required showed an inverse relationship with sCO_2's cycle efficiencies.

Keywords: Concentrated solar power, solar energy, parabolic trough, supercritical Brayton cycle, membrane desalination, direct contact membrane distillation.

NOMENCLATURE

Abbreviations	
CSP	Concentrated solar power
PTC	Parabolic trough solar collector
DCMD	Direct contact membrane distillation
SR	Split Ratio

Symbols	
C_f & C_p	Feed and permeate seawater concentration.
Q_{u_total}	Total heat absorbed by PTSC and input to cycle
Q_u	Heat absorbed by a single unit of PTC
$A_{a,total}$	Total aperture area of the PTC plant
A_a	Aperture area of a PTC unit
Q_{total}	Total solar energy reflected by the collector
E_s	Maximum exergy available on the collector

1. INTRODUCTION

Energy sustainability and water scarcity present significant challenges for the 21st century. Energy scarcity threatens to reduce our quality of life, while carbon emissions pose catastrophic future risks. A lack of clean water affects around 1 in 3 people [1], and 33 countries are at extreme risk regarding clean water supply [2]. Solar energy, particularly Concentrated Solar Power (CSP), emerges as a promising solution to energy sustainability, yet its competitiveness is hindered by current limitations on working fluid, which in turn restricts maximum temperature and theoretical efficiency according to the Carnot cycle. Supercritical fluid has emerged as one potential solution to this problem. Despite potential challenges, a direct CSP system could increase efficiency by eliminating losses in the heat exchanger.

In the field of water desalination, leading-edge methods are generally divided into two categories: membrane-based and thermal-based processes. The most prevalent desalination approach utilizes reverse osmosis, a membrane-based system that demands

This is a paper for 15th International Conference on Applied Energy (ICAE2023), Dec. 3-7, 2023, Doha, Qatar.

significant energy input. Conversely, thermal-based desalination, employed in power plants worldwide, relies on technologies such as Multi-Effect Distillation (MED) and Multi-Stage Flash (MSF). Recently, Membrane Distillation (MD), a novel hybrid technology, has emerged, combining features of both membrane and thermal approaches. The Direct Contact Membrane Distillation (DCMD) variation is particularly noteworthy for its use of low-grade heat and minimal power, distinguishing it from traditional systems, with simplicity as its main advantage. Past research has shown that the combination of these technologies for the poly-generation of water and power is financially viable, even using the conventional Rankine cycle [3]. This research aims to examine the thermodynamic performance of a novel integrated system that combines solar energy collection through parabolic trough collectors with a supercritical carbon dioxide Brayton cycle and desalination by DCMD, marking a novel approach in the field.

2. METHODOLOGY

2.1 Material and methods

Figure 2 illustrates the proposed system. Initially, the supercritical fluid is heated from state 5 to state 3 using a parabolic trough plant, with the energy from the heated fluid being harnessed by the turbine for power generation. Following this, the fluid is employed by the High Temperature Recuperator (HTR) and Low Temperature Recuperator (LTR) to recover the heat of the fluid on the low pressure side. At point 6, the fluid is divided; one portion moves to compressor 2 while the other goes to the cooler, and then to compressor 1. This division of fluid allows for more effective heat transfer utilization, due to the significant specific heat capacity of supercritical fluid near its critical point. In this setup, the fluid is cooled by a cooler from point 6 to 1, with the heat being absorbed by seawater to produce clean water through Direct Contact Membrane Distillation (DCMD). The fluid at points 2 and 10 merge at point 8, and after absorbing heat at HTR, which acts as a preheater, the fluid goes to the parabolic trough plant, and the cycle begins again.

An integrated math-model was coded into the Engineering Equation Solver (EES). The Brayton cycle configuration is a recompression cycle, and its operating conditions, under a nameplate capacity or design specifications, are 50 MW_{net}@ DNI of 1000 W/m^2. The design conditions for the cycle are represented in Table 1. The mass flow rate was determined by using the parametric table of EES that corresponds to 50MW_{net} and maintaining approach temperatures of 10K for HTR and 5K for LTR to ensure both HTR and LTR can properly operate under a large heat load as mentioned in [4].

For the parabolic trough plant, the entire power plant was modelled as a single large-scale heater, simplifying the analysis of the cogeneration system. The parabolic trough solar power plant was conceptualized as a unique heat exchanger, absorbing solar radiation to heat a working fluid. This approach reduced complexity while preserving essential thermodynamic characteristics. The power plant was expanded from a single modified unit into a unified large-scale heater (refer to equations 1 until 4), and the total reflector area was calculated based on predefined capacity. The limitation of this research method is discussed in section 4.0. The aperture area of the plant was calculated by determining the heat transferred by the parabolic trough into the cycle $Q_{u,total}$ and the fixed temperature at T5. T5, which is the inlet of the parabolic trough, is fixed at 650K, and the mass flow rate of 2.5 kg/s were chosen due to past research identifying it as the most robust inlet temperature and flow rate [5]. Once $Q_{u,total}$ was calculated, the total aperture area of the parabolic trough can be calculated by equations 1 and 2. A slightly modified LS-3 parabolic trough was used to allow it to withstand the high pressure of the fluid, and the full specification can be found at [6].

The DCMD module had an operative membrane area of 0.56 m², achieved by stacking four layers of 0.2m by 0.7m membrane sheets [3]. The feed and permeate were directed to flow in counter directions to increase the permeate flux. The operating conditions of direct contact membrane distillation are shown in Table 2. The research assumed negligible pressure variations in the sCO2 cycle except at turbines and compressors, constant isentropic efficiency, and no effects of potential and kinetic energy. The DCMD system presumed uniform membrane pore size, ignored surface diffusion due to hydrophobicity, and static air in the pores. Moreover, it is worth mentioning that the control system is not within the paper's scope.

Table 1. The inputs and fixed conditions of sCO_2 Brayton cycle [7] [8]

Temperature at the inlet of compressor 1	304.25K
Pressure at the inlet of the compressor 1	7.4MPa
Pressure ratio	2.7
High temperature recuperator effectiveness, HTR	0.85
Low temperature recuperator effectiveness, LTR	0.7
Isentropic efficiencies of the compressors	0.8
Isentropic efficiencies of the turbines	0.9
Split Ratio (SR)	Variable
Temperature, state 5 (T5)	650K
Mass flow rate (kg/s)	628 kg/s

Table 2. Input conditions and characteristics of DCDM module [3]

Description	Parameter	Value / Type
Membrane properties	Sheet type	Flat Sheet
	Material	PTFE
	Length	0.7 m
	Width	0.2 m
	Thickness (height)	0.001 m
	Effective area of membrane	0.56 m^2(0.14m^2 each layer)
	Membrane Pore δ_m	120 μm
	Porosity ε	0.91 (91 %)
	Tortuosity	1.098
	Thermal conductivity K_m	0.2 W/m*K
Operating conditions	C_f	0.35 g/kg
	C_P	0
	Feed flow rate	20 L/min
	Permeate flow rate	20 L/min

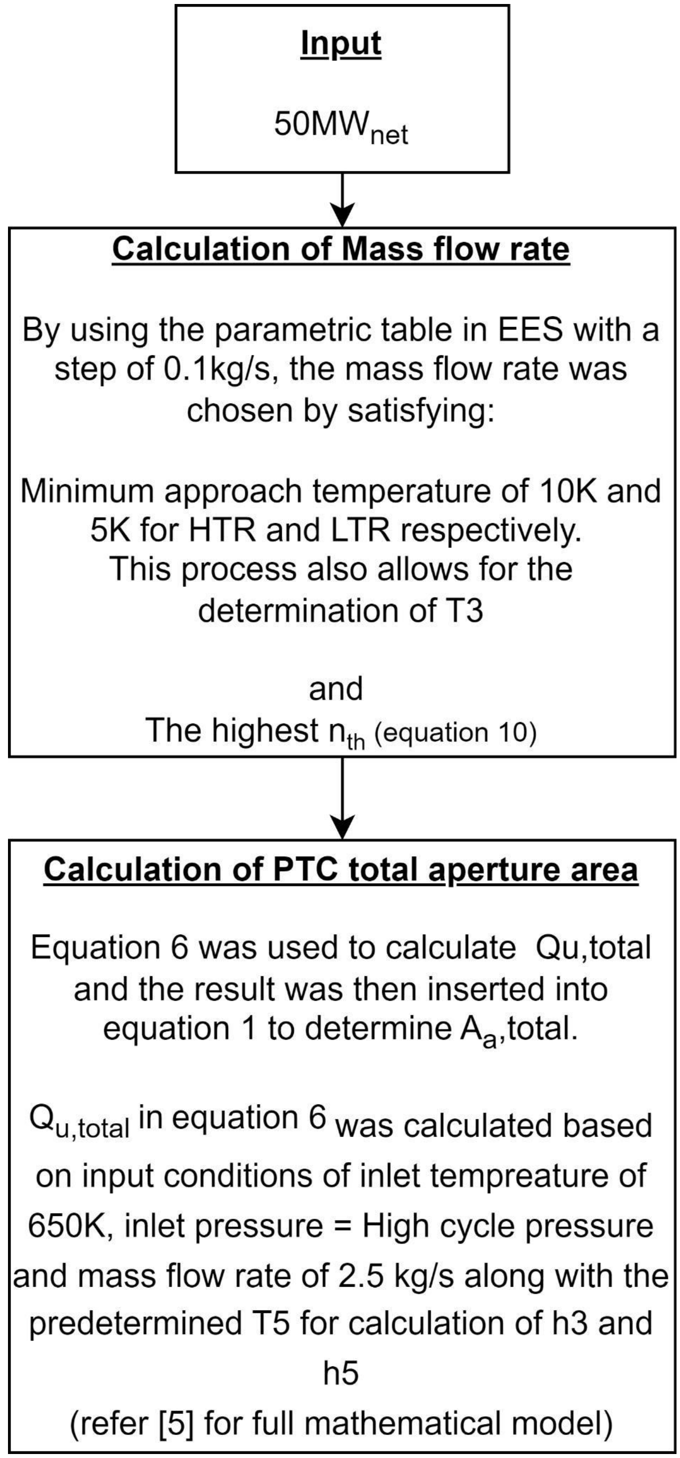

Fig. 1. Calculation procedure for total aperture area ($A_{a,total}$) of PTSC plant

2.2 Mathematical model

The mathematical model of the integrated model is shown in Figure 2. For PTSC model the full mathematical model and nomenclatures are shown in [5]. The process of increasing the size of a single unit of PTSC model to a unified large heater for thermal and exergetic are:

$$Q_{u\_total} = \left(\frac{Qu}{A_a}\right) * A_{a,total} \quad (1)$$

$$Q_{total} = I_b * \eta_0 * A_{a,total} \quad (2)$$

$$E_{u.total} = \frac{E_u}{A_a} * A_{a,total} \quad (3)$$

$$E_s = I_b * A_{a,total} * \left[1 - \left(\frac{4}{3} * \frac{T_{amb}}{T_{sun}}\right) + \left(\frac{1}{3} * \left(\frac{T_{amb}}{T_{sun}}\right)^4\right)\right] \quad (4)$$

For the recompression sCO_2 Brayton cycle, the calculation was carried out using common thermodynamic methods, including isentropic efficiency measurements for turbines and compressors, and principles of energy balance and effectiveness for HTR and LTR that can be seen in [7]. In addition, a governing equation of the SR at point 8 in the system is given as:

$$h_8 = [(1 - SR) * h_{10}] + (SR * h_7) \quad (5)$$

The heat input form the PTSC field to the cycle is:

$$Q_{u,total} = \dot{m} * (h_3 - h_5) \quad (6)$$

For the DCMD process, an iterative method was used. Initially, the membrane feed and permeate temperatures were assumed to be the same as the bulk temperature in order to calculate the permeate flux of the DCMD unit. The full method and equation for this iteration can be found in reference [9]. The amount of heat rejected by the Brayton cycle and absorbed by the seawater at condenser is given by

$$Q_{out} = \dot{m}_{sea} * (h_{12} - h_{11}) \quad (7)$$

The total number of DCMD units required is determined by the amount of $\dot{m}$ needed, and it can be computed according to the equation below:

$$N_{DCMD} = \dot{m}_{sea} \ / \ \dot{m}_{DCMD} \quad (8)$$

With $\dot{m}_{DCMD}$ representing the mass flow rate for each unit of DCMD, the value of $\dot{m}_{DCMD}$ is 0.333 kg/s. This was determined by converting from the inlet volumetric flow rate of 20 L/min, as shown in table 2. The volume of water produced for each unit of DCMD, measured in cubic meters per hour, is:

$$V_{\text{water}} = A_{DCMD} * J_{mh} / \rho_{\text{water}} \quad (9)$$

Since the system is directly integrated, it is most fitting to consider the index of the overall system instead of individual component. The energetic and exergetic efficiency is thus calculated accordingly.

$$\eta_{th} = \frac{w_{net}}{Q_{total}} \quad (10)$$

$$\eta_{ex} = \frac{w_{net}}{E_s} \quad (11)$$

Please note the model above was validated to maintained accuracy. Moreover, for a comprehensive schematic diagram of the system, including the location and numbering of each state, please see Fig. 2

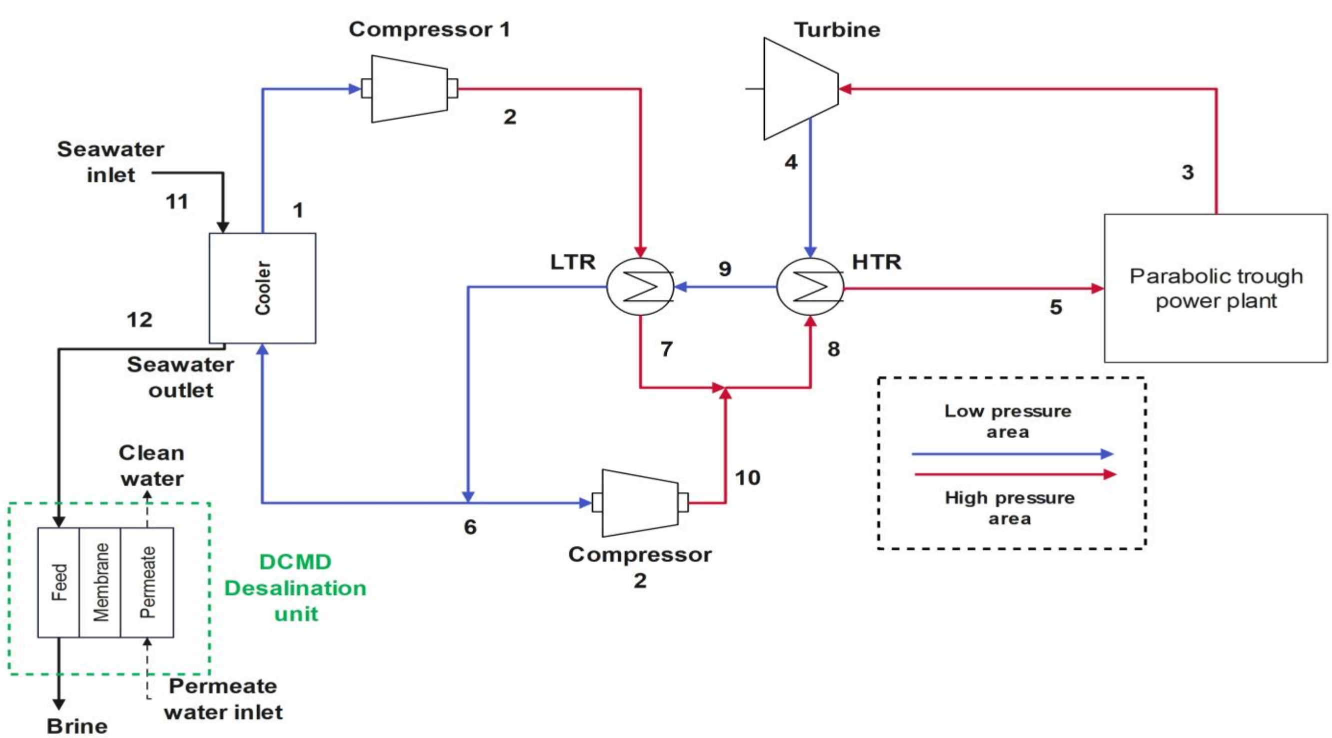

Fig. 2.Schematic layout of a direct parabolic trough - sCO_2recompression Brayton cycle with DCMD desalination.

3.0 Results and discussion

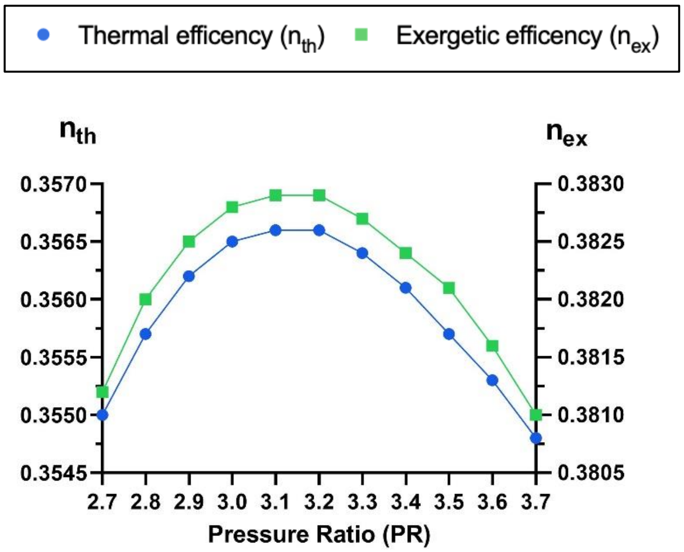

Fig. 3. Relationship between pressure ratio with thermal and exergetic efficiency

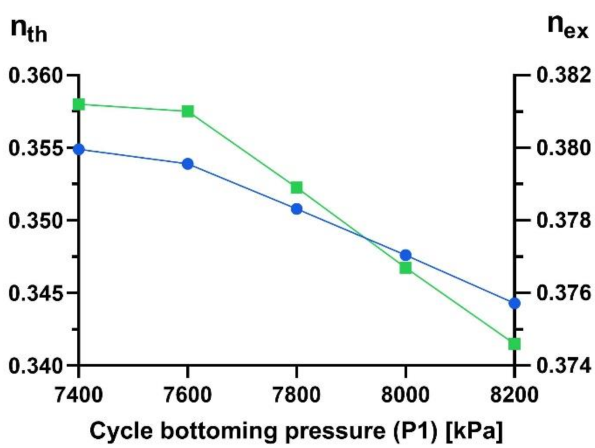

Fig. 4. Relationship between bottoming pressure (P1) with thermal and exergetic efficiency

Figure 3 and 4 illustrate the relationship between various PRs and the cycle bottoming pressure with energetic/thermal (η_{th}) and exergetic efficiency (η_{ex}) respectively. Figure 3 shows that initially, an increase in PR leads to higher efficiencies. The reason is that as the Pressure Ratio (PR) rises, the turbine work ($W_{turbine}$) correspondingly increases. However, beyond a value of 3.2, the work required by the compressor exceeds the increment of turbine output, resulting in a reduction in both efficiencies. For instance, the change in net work output (ΔW_{net}), calculated as the difference in turbine output power minus compressor input power between each PR, exhibits a diminishing trend with an increasing Pressure Ratio (PR). Specifically, the ΔW_{net} is 101 kW when PR increases from 2.7 to 2.8, and this value diminishes to 7 kW as PR further increases from 3.1 to 3.2, reflecting a reduced rate of increment in thermal and exergetic efficiencies as PR rises. However, as PR ranges from 3.2 to 3.7, this trend reverses. The ΔW_{net} transitioning to negative values, going from -1 kW to -74 kW, indicating an amplified rate of reduction in efficiencies, showcasing an increasing rate of efficiencies reduction with rising PR.

Bottoming cycle showed a straight forward relationship of continuous reduction as the bottoming cycle increases. The decrease in performance occurs as the difference in pressure between the high and low cycle pressure narrows, causing a reduction in the power output from the turbine. Notably, only a minor decline in performance was detected when the pressure ranged from 7400 to 7600 kPa. This can be explained by the fact that as the value of P1 gets closer to the critical point, the density of supercritical carbon dioxide (sCO_2) increases, thereby lessening the load on the compressor. As the situation moves further from the critical point, the problem becomes more pronounced due to the diminishing density.

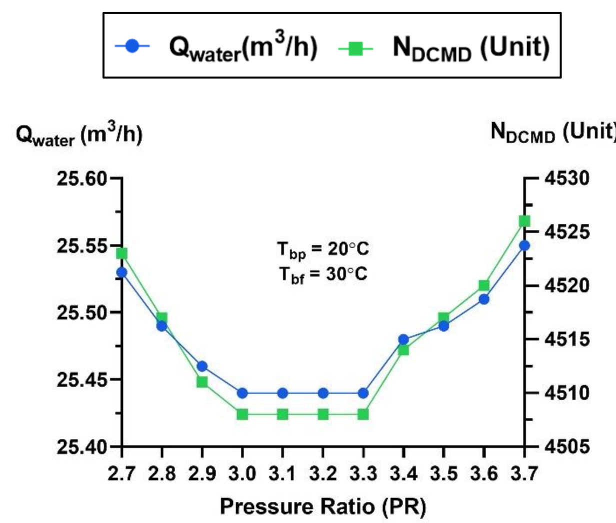

Fig. 5. The relationship between Pressure ratio (PR), total water production(Q_{water}) and Number of DCMD units needed (N_{DCMD})

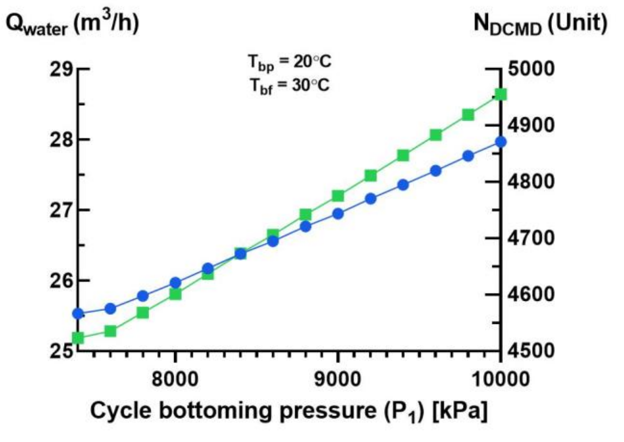

Fig. 6. The relationship between bottoming pressure (P1), total water production(Q_{water}) and Number of DCMD units needed (N_{DCMD})

Figure 5 and 6 show the relationship between various PRs and bottoming cycle (P1) with total water production(Q_{water}) and number of DCMD units needed (N_{DCMD}) respectively. The results in Figure 5 shows that it decreases until reaching minimum point and subsequently increases with PR. The phenomenon observed can be explained by the concepts outlined in Figure 3, where the thermodynamic performance increased with the Pressure Ratio (PR) until it reached a peak, and then began to decrease. This enhancement in performance indicates a more effective use of heat in the sCO_2 cycle. As the cycle utilizes more heat, a smaller amount heat remains accessible to the seawater at the cooler for the desalination process, thereby limiting its maximum water production capability and the unit of DCMD required, and the reverse is also true. The maximum water produced (Q_{water}) and units needed (N_{DCMD}) was observed at PR of 3.7 with 25.55 m^3/h and 4526 units respectively.

Figure 6 depicts that the correlation is evident: as the value of P1 increases, the efficiency of the cycle diminishes resulting in more heat being left unused by the cycle. This surplus heat is then taken up by the seawater, leading to a higher necessary mass flow rate albeit with the trade-off of reduced power generation. Therefore, a decision to raise P1 should be made with caution, and only if the priority lies in enhancing water production. However, it is worth mentioning that the slope value for Q_{water} is lower than N_{DCMD} with around 0.0009385 and 0.166 respectively. Consequently, increasing PR leads to more units needed with diminishing rate of return on water production.

4.0 Research limitations

The assumption that treats the entire parabolic trough power plant as one heater by super scaling an individual unit overlooks the specific effects of individual trough configurations, possibly overestimating heat absorption. While we apply these simplifications consistently, ensuring valid comparative analysis, the approach may lack precision in evaluating specific component design. This method offers valuable insights for comparative studies but falls short for detailed predictions of parabolic trough plant performance. Future research could enhance this work with more detailed models considering the configuration and designs of the plant.

5.0 Future direction of this research

The future direction of this preliminary research is by conduction a detailed analysis of the system at wide-scale combinations of operating conditions and with a focus on temperature polarization phenomena on DCDM and its impact on the system's performance.

6.0 Conclusions

The aim of this research is to evaluate the performance of a novel integrated parabolic trough power plant, sCO_2 recompression Brayton cycle and direct contact membrane distillation system for the co-generation of power and water. By using an integrated mathematical model coded in engineering equation solver (EES), we derived several key insights:

1) Thermal and exergetic efficiency rises with Pressure Ratio (PR) around 3.2, then falls. The bottoming cycle continuously reduces efficiency, with minor declines between pressures of 7400 to 7600 kPa due to sCO2 density changes near the critical point.

2) The relationship between pressure ratio (PR) and the bottoming cycle (P1) impacts water production and DCMD units needed. The results showed that the amount of water production and unit of DCMD needed have an inverse relationship with thermal and exergetic efficiencies. This reflects the heat utilization in the sCO_2 cycle, influencing the water production capacity.

ACKNOWLEDGEMENT

We would like to thank The Hong Kong Polytechnic University for their financial support.

REFERENCE

[1] UNICEF. 1 in 3 people globally do not have access to safe drinking water – UNICEF, WHO New york, Geneva2019. Retrieved from: https://www.who.int/news/item/18-06-2019-1-in-3-people-globally-do-not-have-access-to-safe-drinking-water-unicef-who. (retrieved on 10.08.2023)
[2] Andrew Maddocks RSYaPR. Ranking the World's Most Water-Stressed Countries in 2040 20115. Retrieved from: https://www.wri.org/insights/ranking-worlds-most-water-stressed-countries-2040. (retrieved on 10.08.2023)
[3] Soomro MI, Kim W-S. Parabolic-trough plant integrated with direct-contact membrane distillation system: Concept, simulation, performance, and economic evaluation. Solar Energy. 2018;173:348-61.
[4] Linares JI, Montes MJ, Cantizano A, Sánchez C. A novel supercritical CO2 recompression Brayton power cycle for power tower concentrating solar plants. Applied Energy. 2020;263:114644.
[5] Zaharil HA. An investigation on the usage of different supercritical fluids in parabolic trough solar collector. Renewable Energy. 2021;168:676-91.
[6] Zaharil HA, Yang H. A fundamental investigation on supercritical carbon dioxide energetic, exergetic and entropy behavior in parabolic trough solar collector. Journal of Cleaner Production. 2023;384:135625.

[7] Al-Sulaiman FA, Atif M. Performance comparison of different supercritical carbon dioxide Brayton cycles integrated with a solar power tower. Energy. 2015;82:61-71.
[8] Chacartegui R, Muñoz de Escalona JM, Sánchez D, Monje B, Sánchez T. Alternative cycles based on carbon dioxide for central receiver solar power plants. Applied Thermal Engineering. 2011;31(5):872-9.
[9] Olatunji SO, Camacho LM. Heat and Mass Transport in Modeling Membrane Distillation Configurations: A Review. Frontiers in Energy Research. 2018;6.